Intelligent Nanorobots

DOI: 10.1002/anie.201202044

Fantastic Voyage: Designing Self-Powered Nanorobots

*Samudra Sengupta, Michael E. Ibele, and Ayusman Sen**

chemotaxis · collective behavior · micropumps · nanomotors · nanorobots

The use of swarms of nanobots to perform seemingly miraculous tasks is a common trope in the annals of science fiction.[1] Although several of these remarkable feats are still very much in the realm of fiction, scientists have recently overcome many of the physical challenges associated with operating on the small scale and have generated the first generation of autonomous self-powered nanomotors and pumps. The motors can be directed by chemical and light gradients, pick up and deliver cargo, and exhibit collective behavior.

1. Introduction

It is often said that we are living in the information age, a time when the innovations in society and technology are driven by the ability to communicate and integrate ideas. Just as easily, it can be said that we are living in the age of miniaturization, since the ability to fabricate, manipulate, and integrate matter on the very small scale has ushered in this new information age. But, while we have become quite adept at fabricating materials on the small scale and manipulating the flow of electrons through them, the ability to precisely control the motion of the materials themselves, on these micro- and nanoscales is a much more nascent area of research. Until recently, the work was mostly focused on coaxing micro- and nano-electromechanical structures (MEMS and NEMS) to deform and move repeatedly over well-defined small distances.[2] This Minireview focuses on a complementary, and arguably more challenging, avenue of research, namely: How can we design populations of artificial micro- and nanostructures capable of moving autonomously over long distances while at the same time being able to organize themselves on command to perform complex tasks? The potential applications of such highly developed artificial "nanobots" would be limitless, from the real-time reconfiguration of electronic assemblies in order to strategically optimize computing power, to the targeted removal of localized disease components, and the modular repair of individual cellular components.[3]

Indeed, there are continuing efforts to design microrobots for in vivo medical applications.[4] For example, Ishiyama et al. have reported on the design of tiny magnetically driven spinning screws intended to swim along veins and either deliver drugs to target tissues or to embed into tumors and destroy them thermally.[5] Nelson et al. have fabricated microscopic robots (ca. 200 μm) that can be injected into the body. These devices might someday be used for drug delivery or to perform minimally invasive eye surgery.[6] In a slightly different approach, the oxygen requirement has been numerically modeled for chemically powered nanorobots that may travel through the bloodstream utilizing glucose as the fuel. The authors find that robots about 1 μm in size can produce up to several tens of picowatts, in steady state, if they fully use oxygen reaching their surface from the blood plasma.[7]

2. Physical Constraints on Nanomotor Designs

One might think from looking at nature that the design of such motors would be a relatively simple task.[8] In the natural world, the fine-tuned control of motion on the smallest of scales is ubiquitous.[8,9] Many species of micron-sized bacteria swim through solution by using motor proteins, which power the motion of flagella or cilia.[10] Other bacteria move across surfaces by extending and retracting hairlike pili from their cell membranes.[11] Even inside these cells, ions are continuously being pumped against gradients,[12] and chemical information is constantly being transcribed on the nanometer scale.[10]

Evolution, however, has had millions of years of trial and error to perfect these nanomotor designs. Technological advancement, which operates at a significantly faster pace, must take advantage of our ability to intelligently design potential motors. The inherent challenge, however, is that our intuition regarding how physics operates is based on observations of macroscale systems. At the micro- and nanoscales several physical effects, which are quite negligible on the macroscale, begin to dominate. As a result, traditional macroscale motor designs cease to function when scaled

[*] S. Sengupta, Dr. M. E. Ibele, Dr. A. Sen
Department of Chemistry, The Pennsylvania State University
University Park, PA 16802 (USA)
E-mail: asen@psu.edu
Homepage: http://research.chem.psu.edu/axsgroup

down to this size regime, and other motor designs must be employed.

2.1. Scaling Laws

On the macroscale, an object's volume is large compared to its surface area, and as a result, properties related to the object's volume (e.g. mass, inertia) tend to dictate its behavior. As an object is scaled down by a factor of ΔR, however, the volume of the object shrinks by a factor of ΔR^3, whereas the object's surface area shrinks by only ΔR^2. For this reason, surface effects tend to dominate on the small scale. For instance, for small objects the rate at which the object can dissipate energy into its environment, which is proportional to its surface area, becomes large relative to its capacity to store fuel inside itself. As a result, nanoscale particles must actively harness energy from outside sources (e.g. external electric fields,[13] magnetic fields,[14] thermal[15] or chemical gradients,[16] or chemical fuels[17] in their environment), or be resigned to motions, which rapidly dissipate as their on-board fuel supplies are quickly depleted.[18] By the same argument, surface forces also become important at these small scales, as the amount of exposed surface per unit volume becomes relatively large.[19] Thus, a key to powering nanobots is to generate asymmetric surface gradients of various types.

Similarly, when an object is scaled down, Brownian randomization effects become more prominent, since an object's rate of collisions with its surroundings shrinks with its change in surface area, as ΔR^2, whereas its inertia, being proportional to its volume, shrinks much more quickly, as ΔR^3. In addition, because there are fewer total collisions occurring on smaller particles, there is a greater likelihood that the momentum from collisions on opposite sides of the particle may not completely average out over short observation times. As a result, freely moving particles in a fluid tend to move about in a random-walk trajectory. Although one can use statistical arguments to calculate the expected average displacement of such a particle over a given time-frame, arbitrarily precise predictions of its trajectory are impossible. Biological motors have evolved to cope with this complication by actually harnessing and rectifying the energy of these random collisions on their surfaces to allow them to move, instead of fighting against them ("Brownian ratchets").[20]

As is often the case in work with nanoscale objects, not only are the objects themselves miniscule, but so too is the typical spacing between nearby objects. As a result, several physical forces, which are negligible across long distances, begin to dominate on the nanoscale. Electrostatic forces between charged objects, for instance, grow proportional to ΔR^2 as the distance between objects is decreased. The (usually attractive) van der Waals interactions between an object and its neighbors, on the other hand, grow by ΔR^6.

2.2. Fluid Reynolds Number

Another consequence of operating at the micro- and nanoscales is that fluids at these scales behave differently from what our intuition predicts. This is especially important in the discussion of nanomotors because, as mentioned above, most nanomotors must travel through (fuel-enriched) fluids. At these scales, the inertial forces associated with the movement of the motor in the fluid become negligible relative to the viscous drag. Consequently, the Reynolds number (Re) of the particle, which is usually measured as the ratio of inertial to the viscous force [Eq. (1)], becomes very small.

$$\mathrm{Re} = \frac{\rho V^2 L^2}{\mu V L} \tag{1}$$

Here, Re is the Reynolds number, ρ is the density of the fluid, V is the velocity of the particle relative to the fluid, L is the characteristic length scale—usually considered to be the dimension of the particle, and μ is the viscosity of the fluid.

One direct consequence of low Reynolds number is that the turbulent mixing which is so ubiquitous on the macroscale is essentially absent on the microscale, giving way to primarily laminar flows—a property that has been quite gainfully exploited in a vast array of microfluidic devices.

An interesting property of such laminar fluids is that the motions of the fluid and particles in them are time reversible. This property is highlighted in the famous Couette cell

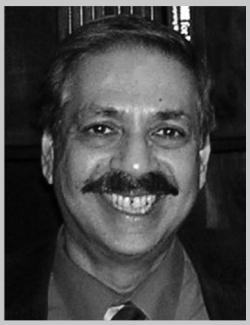

Ayusman Sen was born in Kolkata, India, and received his PhD from the University of Chicago. Following a year of postdoctoral work at the California Institute of Technology, he joined the Chemistry Department of the Pennsylvania State University, where is currently a Distinguished Professor. He is a Fellow of the American Association for the Advancement of Science. His research interests encompass catalysis, organometallic and polymer chemistry, and nanotechnology.

Samudra Sengupta was born in Kolkata, India, and received his MSc in Chemistry from St. Stephen's College, Delhi University, in 2007. He is currently working towards his PhD under the guidance of Prof. Ayusman Sen at the Pennsylvania State University. His research interests include single-molecule studies, and designing new enzyme-based devices. He recently received the Materials Research Institute Fellowship at the Pennsylvania State University.

Michael Ibele earned his BS in Chemistry in 2005 from the University of North Carolina and conducted research on synthetic nanomotors under the tutelage of Professor Ayusman Sen at the Pennsylvania State University (PhD 2010).He is currently an Assistant Professor at Lindenwood University in St. Charles, Missouri.

demonstration, wherein laminar colored fluids between two cylindrical plates are "mixed" by moving one plate relative to the other and then "unmixed" by performing the reverse motion.[21] As a direct consequence of this microscopic reversibility in laminar fluids, it is impossible for any isolated tiny organism or nanorobot to swim through a quiescent low-Reynolds-number fluid by means of a strictly reciprocal conformational motion. A micron-sized scallop-shaped object, for instance, might swim forward by quickly closing its shell but, in a low-Reynolds-number fluid, the act of opening the shell would undo the original translation, no matter how slowly the shell was reopened.[22] This is very different from the macroscopic world where reciprocal motion is commonly employed in motors of various kinds.

2.3. Electrical Double-Layer

The properties of low-Reynolds-number fluids listed above are mainly concerned with bulk fluids. However, any object placed in a fluid will, even if the object is at rest, exert some influence on the fluid at its surface. The van der Waals forces at an object's surface, for example, often pin the first few molecular layers of fluid at the surface, resulting in what is known as a "no-slip" boundary condition. In protic solvents, beyond this pinned layer, but still relatively close to the surface, the electrical properties of the fluid are also different from those in the bulk. In this region, the inherent surface charge of the object attracts oppositely charged ions from the solution to counter it. Thus, it is some distance away from the particle, usually on the order of tens to hundreds of nanometers, before the charge of the particle is appropriately screened, and the fluid composition approaches that of the bulk. The distance over which this screening takes place is described as the object's Debye length (κ^{-1} by convention), which can be calculated from Equation (2).

$$\kappa^{-1} = \sqrt{\frac{\varepsilon_0 \varepsilon_r k_B T}{2 N_A e^2 I}} \qquad (2)$$

Here ε_0 is the permittivity of free space, ε_r is the dielectric constant of the electrolyte, k_B is the Boltzmann constant, N_A is Avogadro's number, e is the charge of an electron, and I is the solution ionic strength. This electrically charged region of fluid surrounding the object, when combined with the pinned layer directly at the object's surface, is often referred to as the object's electrical double-layer.

As Equation (2) shows, the thickness of the double-layer is strongly influenced by the ionic strength of the solution. The Debye length has important implications with respect to particle stability. In solutions containing more ions, the thickness of the double-layer is smaller, and the similarly charged objects can come closer to one another without feeling significant repulsive forces. If the Debye length is too small and this distance becomes too close, then attractive van der Waals forces begin to dominate, leading to particle aggregation.

3. Survey of Artificial Nanomotors

Despite these inherent constraints, recent technological advances have opened the door to the fabrication of micro- and nanoscale artificial motors.[23] One approach to making these motors is to interface artificial components with existing biological motors (Figure 1).[24] In one report, heart muscle cells were hybridized to a polydimethylsiloxane MEMS device, which then gained the ability to move across a surface by a crawling mechanism as the heart cells beat.[25] Similarly, motile bacteria cells have been interfaced with micron-sized beads to propel the beads through solution.[26] One need not

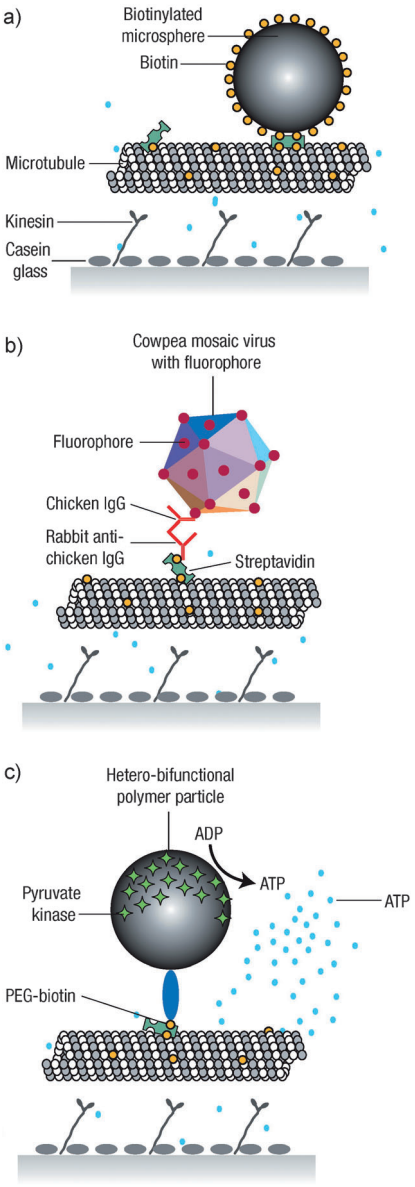

Figure 1. Representation showing the use of molecular recognition for binding specific cargo. A variety of techniques can be used to couple biological and artificial cargo to microtubules like a) the use of avidin or streptavidin to couple biotinylated objects and microtubules; b) tagging cargo with antibodies for biological molecules, viruses, or cells; and c) tethering cargo particles bearing pyruvate kinase to microtubules to provide a local ATP source. From Ref. [24].

even use an entire cell to achieve motion. Individual motor proteins can be extracted from cells and interfaced with artificial devices. A 10 nm motor protein, F1-adenosine triphosphate synthase (F1-ATPase), for example, has been used to rotate micron-sized nickel propellers.[27] The motor protein kinesin has also been used to transport microtubules across surfaces (Figure 2).[28]

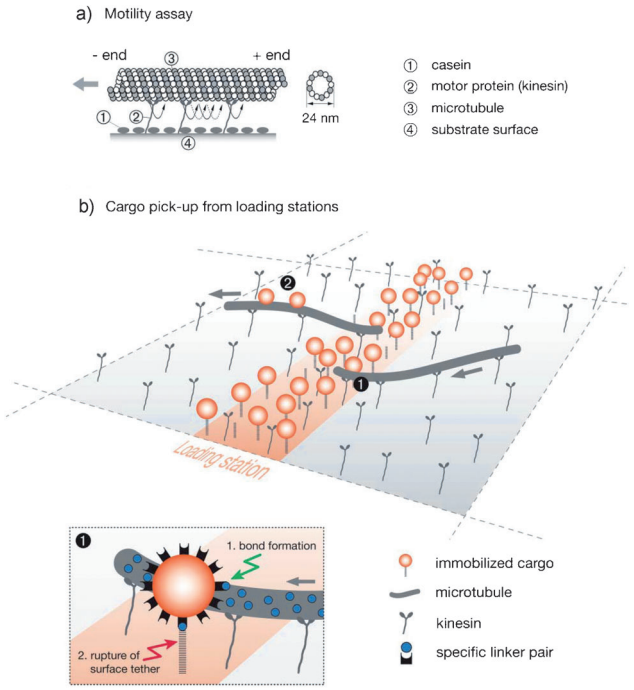

Figure 2. a) Surface-adsorbed motor proteins (kinesin) bind to the functionalized microtubules to power these molecular shuttles. The function of the motors and their filaments are preserved by the casein, which passivates the substrate surface. b) The molecular shuttles move into the cargo-immobilized loading stations to pick up and transport the cargo. Reversible linkers immobilizing the cargo to the surface facilitate the binding of the passing shuttle to the cargo. From Ref. [28].

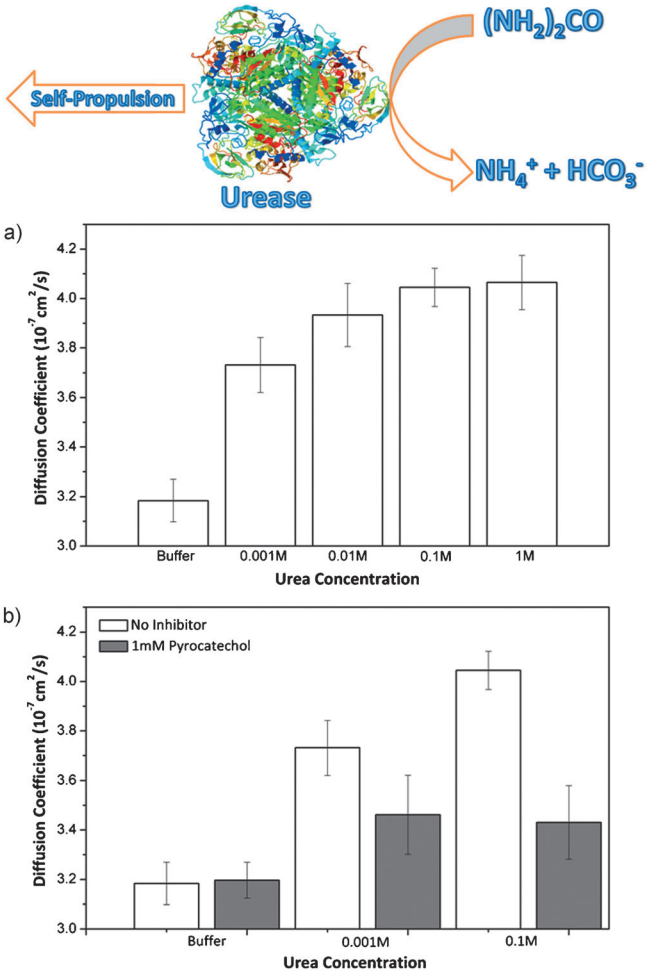

Figure 3. a) The diffusion coefficient of single molecules of urease enzyme increased with increasing urea concentration. b) The enhancement in urease diffusion decreased significantly in the presence of pyrocatechol, a urease inhibitor. From Ref. [30a].

Surprisingly, it is not necessary to use only those cellular enzymes and proteins that are associated with motion. This is especially true when multiple enzymes are incorporated into a single device in a logical manner.[29] Although the mechanisms of motion are still a matter of debate, single-molecule enzymes can potentially induce motion through substrate turnover.[30] For example, Sen and Butler have demonstrated that single-urease enzyme molecules show a substrate-concentration-dependent enhancement in diffusion, which was highly attenuated in the presence of a urease inhibitor (Figure 3).[30a]

The drawback for incorporating biological motors directly into synthetic devices is that each of these motors evolved to work in a specific biological environment and that environment is not necessarily compatible with the device. Electrostatic and van der Waals interactions with the device's supporting surface often cause misfolding of the proteins and loss of catalytic activity.[31] These same forces also lead to nonspecific binding of the proteins and, as a result, the exposed surfaces of the device must be protected from biofouling. In addition, biological motors typically require physiological conditions to operate, and although these conditions can be approximated with the appropriate buffer solution, the relatively high ionic strength of the buffer decreases the thickness of the double-layers around the device, leading to aggregation. One final drawback to biological/artificial hybrid systems is that, in some sense, they do not address the overall goal: the artificial engineering of micro- and nanoscale motors.

Below, we describe the purely synthetic motors that have been reported in the literature. These are classified according to their propulsion mechanism.

3.1. Self-Electrophoretic Motors

Electrophoresis is the movement of charged objects in an electric field. Typically, an electric field is generated across the motor in a fluid. This electric field drives the motion of the charges on the surface of the motor creating a slip velocity

whereby the fluid is allowed to flow around the object. The motor is thus driven in the opposite direction at a velocity U governed by Equation (3).

$$U = \frac{\varepsilon \zeta E}{\eta} \quad (3)$$

Here ε is the dielectric constant of the solution, ζ is the zeta potential of the object, E is the magnitude of the electric field, and η is viscosity.[32]

The first wholly synthetic autonomous nanomotor of this type was synthesized by Mallouk and Sen in 2004 (Figure 4),[33] followed closely by a related system by Ozin et al.,[34] and was modeled after a much larger, millimeter-scale catalytic motor described by Whitesides et al.[35] The Whitesides motor consisted of a polymer disc with a platinum-coated rudder. When this disc was floated on top of an aqueous solution containing H_2O_2, the platinum rudder converted the H_2O_2 into oxygen gas and propelled the entire structure forward by means of a bubble-recoil mechanism. To mimic this system, Mallouk and Sen created a bimetallic nanorod, approximately 2 μm in length and 400 nm in diameter, with a catalytically active platinum end and a (supposedly) inert gold end (Pt–Au micromotors). When placed in aqueous solutions containing H_2O_2, the Pt–Au nanomotors propelled themselves through solution at speeds of approximately 5–10 $\mu m\,s^{-1}$—platinum end first. Although bubbles spontaneously formed elsewhere in solution, no bubbles were observed issuing from the nanorods. Because of this and because the direction of motion of these nanorods was opposite to that which was expected from bubble-recoil mechanism, a new mechanism was required—one that took into account the unique physics of nanoscale objects. The initial hypothesis was that the oxygen generated by the platinum end of the motor lowered the surface tension of the fluid on that end of the rod, and since the gold end of the microrod was hydrophobic (due to pinned nanobubbles), the gold end was pulled towards the more oxygen-rich region of the solution near the platinum end. Although self-generated surface tension gradients have been known to cause motion in other chemical systems,[36] ultimately it was shown that this mechanism played at best only a secondary role in the movement of these nanorods. Instead, the motion of these nanorods is now attributed to the asymmetric decomposition of H_2O_2 across both metallic surfaces of the rod—the platinum which oxidizes H_2O_2 and the gold which reduces it.[17,37] In this mechanism, the decomposition of H_2O_2 sets up a proton gradient along the axis of the microrod in solution, and the negatively charged microrod responds by moving towards the proton-rich solution by a self-electrophoretic mechanism.[38] Using H_2O_2 as the fuel, other bimetallic nanorod combinations have also been shown to move by the same mechanism.[34,38] A very similar mechanism was demonstrated by Mano and Heller for the movement of carbon fibers that were impregnated with glucose oxidase on one end and an oxygen reductase at the other.[29b] It is, of course, interesting to note that proton gradients are responsible for much of the transport in living systems.[39] The concept of motion resulting from ion gradients generated by redox reactions occurring at two ends of an object appears to be quite general (Figure 5). For example, Sen et al. have designed a highly efficient, bubble-free, bimetallic Cu–Pt nanomotor that is powered in Br_2 or I_2 solution (Figure 6).[40] In another example, motion of a metallic object was observed when one end was the site of metal deposition and the other end was the site of metal dissolution.[41]

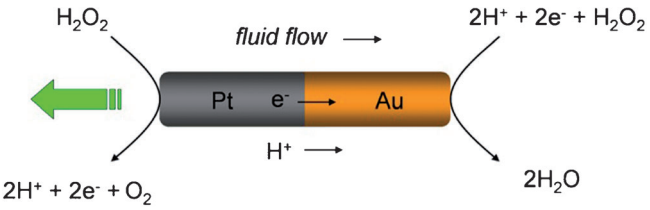

Figure 4. Representation of a bimetallic Pt–Au nanorod powered by the catalytic decomposition of hydrogen peroxide. From Ref. [33].

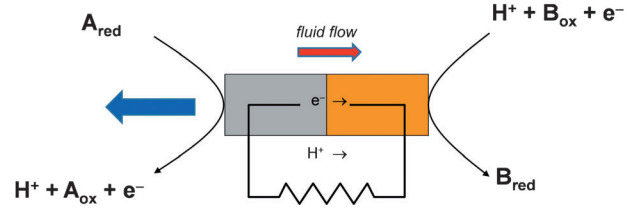

Figure 5. A general mechanism of motion that involves ionic gradients generated by redox reactions occurring at opposite ends of an object. From Ref. [37a].

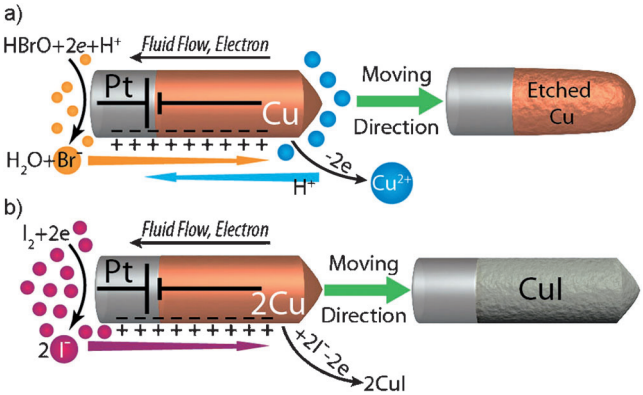

Figure 6. Mechanism behind the motion of bimetallic Cu–Pt nanorods in aqueous solutions of a) Br_2 and b) I_2. From Ref. [40].

Since the inception of bimetallic nanorod motors in 2004, several functionalities and design improvements have been incorporated. Wang's group, in particular, has been instrumental in this regard, showing that the speed of the motors can be increased by incorporating silver metal[42] or carbon nanotubes[43] into the body of the nanorod; by dissolving silver ions in the peroxide solution;[44] by increasing the temperature

of the solution;[45] by modulating the electrical potential of the underlying surface over which the motors travel;[46] by partial dissolution of the central Ag segment to create flexible rods;[47] and by incorporating a flexible Ag segment.[48] Ozin and co-workers have also been instrumental in exploring the properties of these new motors, showing that the speed of the Pt–Au micromotors is proportional to the roughness of the motor surface.[49]

Expanding on their own work involving the dependence of motor speed on silver ion concentration, the Wang group has also devised a system to detect the binding events of silver-labeled complementary DNA by monitoring the speed of the micromotors (Figure 7).[50]

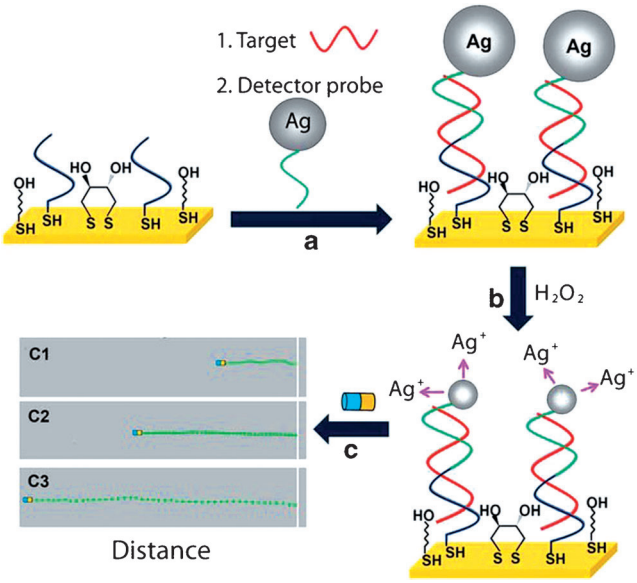

Figure 7. Motion-based detection of nucleic acid involves a) the capture of the Ag-nanoparticle-tagged detector probe on the surface; b) the dissolution of silver nanoparticle tags in the peroxide solution (fuel) to form to a Ag^+-enriched fuel; and c) the detection of the motion of the catalytic nanomotors in the resulting Ag^+-enriched fuel. From Ref. [50].

Ordinarily, Brownian forces exert torque on these microrods causing reorientation, leading to motors that move in powered random-walk-type trajectories over extended time scales. By incorporating short nickel segments into the rod design, Mallouk and Sen showed that the motors can be steered with an externally applied magnetic field.[51] These magnetically steerable motors have also been modified to be able to transport[52] and release[52a,53] micron-sized cargo beads, and to write on the surface of microstructures.[54] Selective capture and transport of biological proteins, and their controlled release have been reported.[55] The arrangement of the metals has also been tailored to generate new motor geometries. This includes the fabrication of "microgears" that rotate in hydrogen peroxide solutions.[56] In addition, Mallouk and co-workers have shown that a thin layer of metal deposited along the length of an existing motor imparts an electrokinetic torque on the motor, turning the translating motor into a stationary micro-rotor (Figure 8).[57]

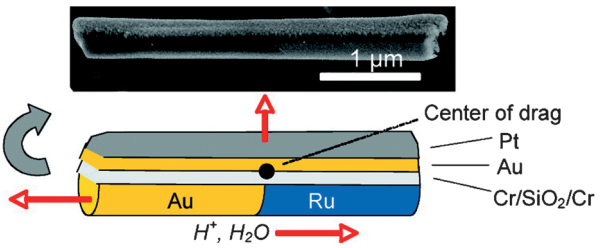

Figure 8. Trimetallic catalytic micromotors fabricated by electrodeposition of cylindrical Au–Ru rods, followed by sequential deposition of Cr, SiO_2, Cr, Au, and Pt on one side of the nanorods. These micromotors rotated rapidly with minimal orbital or translational movement. From Ref. [57b].

Other motor geometries have, of course, been employed in addition to the original cylindrical geometry. That particular shape was chosen initially because of the simplicity with which rods of various compositions can be quickly fabricated[58] and in consideration of the decreased Brownian rotation of the rods owing to rotational drag forces. Janus (two-faced) spheres are also easy structures to fabricate and have been employed as micromotors. These spheres can be made by preparing a monolayer of uniform microspheres on a glass microscope slide, loading the desired metal onto the exposed side of the sphere by vapor-phase deposition, then releasing the spheres through sonication.[59] Several groups have used this method to fabricate Janus motors which move in H_2O_2 and which consist of an inert microsphere capped with a platinum half-shell.[60] These Janus motors can be steered with a magnetic field for pick-up, transport, and delivery of cargo.[60d] Likewise, Zhao and co-workers designed Janus motors with silica heads and TiO_2 arms, which spin[61] and move[62] in H_2O_2. Since many of these motors involve a single metal, the mechanism may involve bubble propulsion or non-electrolyte diffusiophoresis described below (see Sections 3.2 and 3.3).

3.2. Bubble Propulsion

Another way to create motion is by bubble propulsion. Motors that utilize this type of motion create bubbles on their catalytic side and the force from the release of the bubbles causes the motion. This is a gradientlike mechanism since bubbles need to be generated on one side and not the other so there is a change in bubble concentration with distance. Larger, hollow, rod-shaped micromotors have also been fabricated, which are made by rolling up lithographically patterned gold and platinum layers into a microtube-like structure, and swim in H_2O_2 solutions (Figure 9).[63] Sanchez and co-workers attached catalase enzyme on rolled up titanium–gold microtubes, which are also propelled by the catalytic decomposition of H_2O_2 (Figure 10).[64] Because the catalyst (platinum or enzyme) is on the interior of the device, the oxygen produced by the reaction has a hindered diffusion and a favorable place to nucleate, and as a result these motors actually move by a bubble-recoil mechanism. These tubes have been modified to be driven magnetically,[65] act as water-

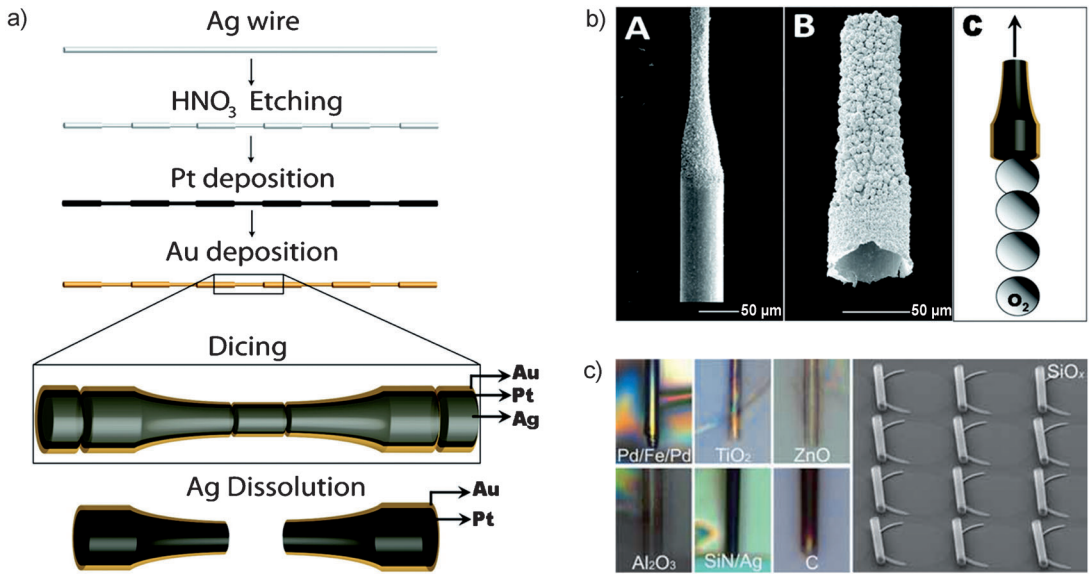

Figure 9. a) The steps involved in the template-assisted preparation of tubular microengines: preparation of the Ag template, electroplating of the Pt and Au layers, dicing of the coated wire, and dissolution of the Ag segment. b) SEM images of A) etched Ag wire 50 μm in diameter, B) a Pt–Au tubular microengine after the Ag dissolution, and C) O_2 bubbles generated from the catalytic decomposition of H_2O_2, which are ejected from the microrocket thereby powering the motor. c) Optical images of different rolled-up nanomembranes, and a SEM image of an array of rolled-up SiO/SiO_2 nanomembranes. From Ref. [63].

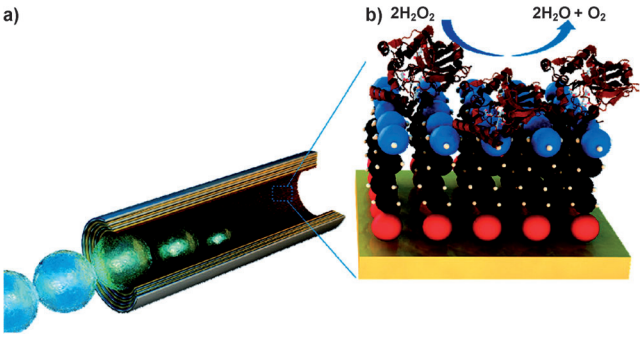

Figure 10. a) View inside the biocatalytic microengine in which catalase enzyme is covalently attached to the inner surface within the rolled-up microtubes. b) Surface modification of the inner Au layer and the enzymatic decomposition of hydrogen peroxide (fuel). From Ref. [64].

striders,[66] function as micropumps,[67] and serve in the controlled capture and release of cargo.[68] The Wang group designed sensing devices that can selectively isolate specific nucleic acids[69] and cancer cells[70] from complex biological mixtures and transport them (Figure 11). Recently, Schmidt and Sanchez reported the smallest microengines, which can be modified to be driven magnetically for pick-up and delivery of cargo to desired locations.[68c] Because of to their unique corkscrew-like trajectory, these artificially powered nanomotors can drill into biomaterials like cells (Figure 12). Further, the efficiency of these microtubes can be tuned by controlling the temperature;[71] through illumination by a white light source;[72] and by membrane template deposition of polyaniline.[73] Movement by bubble-propulsion has also been demonstrated by the Feringa[29c] and Chattopadhyay groups.[74]

3.3. Propulsion by Electrolyte Diffusiophoresis

Another powerful transport mechanism is electrolyte diffusiophoresis. This mechanism is in effect when a gradient of electrolytes is formed across a charged surface. For diffusiophoresis near a wall, there are two effects contributing to the movement of a particle: an electrophoretic effect and a chemophoretic effect, and the speed of the diffusiophoretic movement can be approximated by Equation (4).[75]

$$U=\underbrace{\left[\frac{\mathrm{d}\ln C}{\mathrm{d}x}\right]\left[\frac{D_C-D_A}{D_A-D_C}\right]\left[\frac{k_BT}{e}\right]\left[\frac{\varepsilon(\xi_p-\xi_w)}{\eta}\right]}_{\text{electrical field term}}+\underbrace{\left[\frac{\mathrm{d}\ln C}{\mathrm{d}x}\right]\left[\frac{2\varepsilon k_B^2T^2}{\eta e^2}\right]\left\{\ln\left[1-\tanh^2\left(\frac{e\xi_w}{4k_BT}\right)\right]-\left[1-\tanh^2\left(\frac{e\xi_p}{4k_BT}\right)\right]\right\}}_{\text{chemophoretic term}} \quad (4)$$

Here U is the particle velocity, k_B is the Boltzmann constant, T is temperature, η is the viscosity of the solution, e is the charge of an electron, $\mathrm{d}\ln C/\mathrm{d}x$ is the gradient of the electrolyte, D_C is the diffusion coefficient of the cation, D_A is the diffusion coefficient of the anion, ζ_p is the zeta potential of particles, and ζ_w is the zeta potential of the wall. As shown in Equation (4), electrophoresis results from a difference in diffusivity between the cation and anion, which contributes to the ion gradient in a given direction. This difference leads to a net electric field, which acts both electrophoretically on the nearby particles and osmophoretically on the ions adsorbed in the double-layer of the wall. Also, the concentration gradient of the electrolytes causes a gradient in the thickness of the

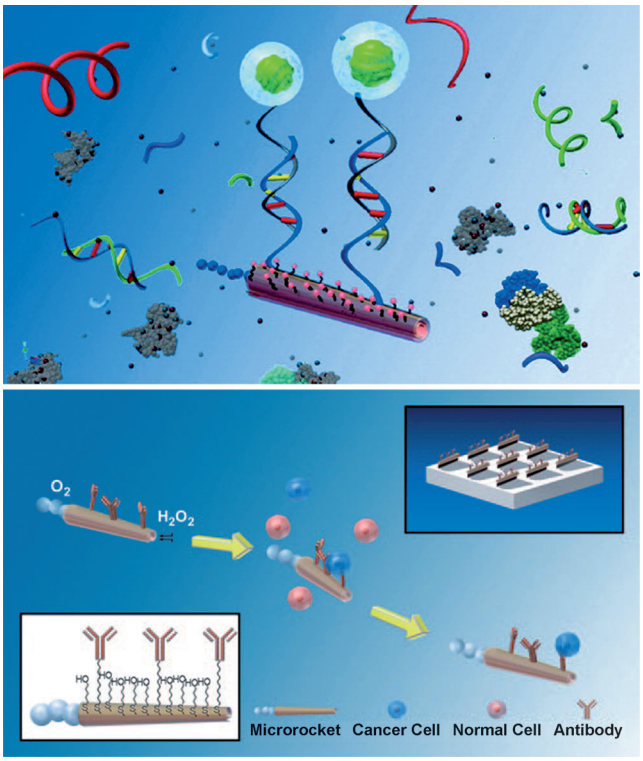

Figure 11. Top: Representation of the motion-based selective capture of the target nucleic acid from a biological sample utilizing a capture-probe-modified nanobot. Bottom: Representation of the selective capture and isolation of cancer cells using microrockets. From Refs. [69, 70].

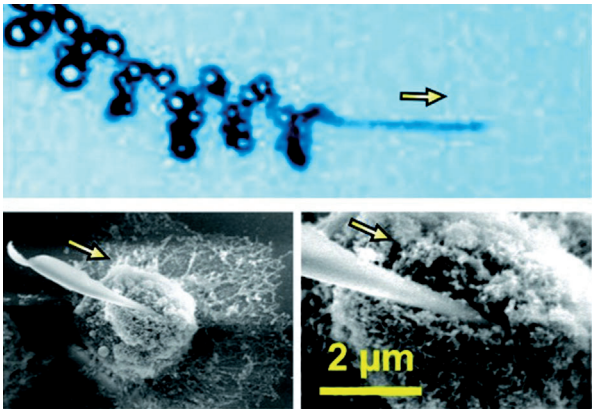

Figure 12. Top: Hollow rolled-up microtubes powered by the catalytic decomposition of hydrogen peroxide moving in a corkscrew-like trajectory. Bottom: SEM images showing that the microengines can drill into fixed cells. From Ref. [68c].

electric double-layer, and thus a "pressure" difference along the wall is created. As a result, the solution will flow from the area of higher electrolyte concentration to that of lower concentration; this is known as the chemophoretic effect. The combination of electrophoretic and chemophoretic effects leads to an overall diffusiophoretic flow, which powers the movement of particles. When the neighboring particles are close enough, the diffusiophoretic flow that is caused by the chemical concentration gradient pushes/pulls nearby particles away/towards the active particle, leading to different kinds of emergent collective behavior, such as chemotactic schooling and predator–prey behavior.[76] Such collective behavior may facilitate the design of novel reconfigurable materials. Sen and co-workers reported a micromotor system in which silver chloride microparticles form "schools" when exposed to UV light (Figure 13).[76,77] These particles can form assemblies that are reversible both in time and space. The emergent collective

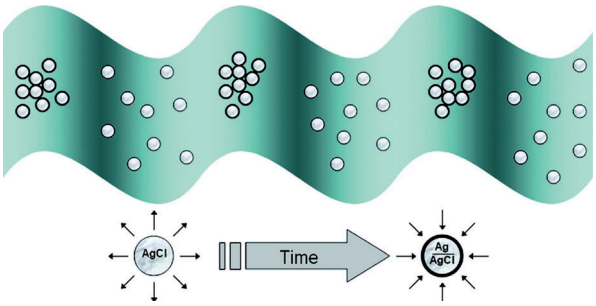

Figure 13. Representation depicting the reversible schooling behavior of silver chloride microparticles in the presence of UV light. From Ref. [77].

behavior of micro/nanoscale active particles was explained by a self-diffusiophoretic mechanism.[78] Each active particle "secretes" chemicals (cations and anions) that serve as signals to other nearby particles. In the presence of both UV light and an oxidant, collective oscillations in their motion arise.[77] The collective motions of these powered nanoparticles result in their self-organization into clumped oscillators with significant spatiotemporal correlations between the clumps. A variant of this system using a regular array of lithographically patterned silver disks supports the propagation of binary "On/Off" Ag/AgCl waves through the lattice.[77] The Sen group has also designed a motor system, which utilizes the photocatalytic properties of titania particles to generate motion and reversible schooling.[79] Similar collective behavior properties of gold nanoparticles, driven by hydrogen peroxide and hydrazine, have been reported by Wang et al.[80] Finally, Sen and Velegol have fabricated asymmetric motors that can also swim in H_2O_2 and exhibit "phototaxis" in UV light.[81]

3.4. Propulsion by Non-Electrolyte Diffusiophoresis

Non-electrolytic diffusiophoresis is movement which is caused by a gradient of uncharged solutes across a surface. These solutes interact with the surface with a certain potential which is determined by the Gibbs' absorption length, K, and the length of the particle–solute interaction, L. The overall equation that defines the velocity of a particle in the gradient is Equation (5).

$$U = \frac{kT}{\eta} KL\nabla C \tag{5}$$

Here k is the Boltzmann constant, T is the temperature of the solution, η is the solution's viscosity, and ∇C is the concentration gradient of the solute.[78] The direction of particle movement depends on whether the particle–solute interaction is repulsive or attractive. Thus, the osmophoretic mechanism in the context of the catalytic motor functions by either creating or depleting more molecules on one side compared to the other, thereby creating an osmotic force around the motor.[60c,82] As an example, Sen et al. fabricated a polymerization-powered Janus motor, the first of its kind outside biological systems (Figure 14).[83] Powered by ring-opening metathesis polymerization (ROMP), these "micro-

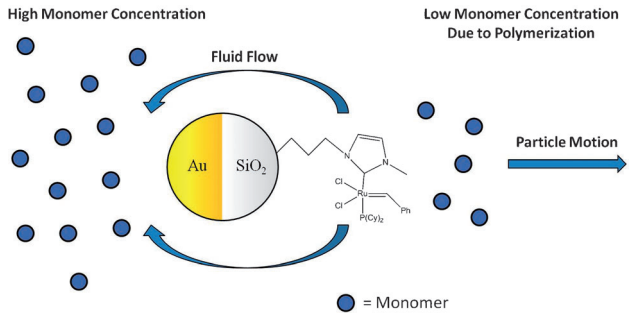

Figure 14. Polymerization-powered Janus motor consumes fuel (monomer) at a silica surface that is functionalized with Grubbs' catalyst, thereby propelling the motor. From Ref. [83].

spiders" utilize Grubbs' catalyst that is asymmetrically immobilized on silica microspheres. Unlike their rod-shaped progenitors, these spheres rotate fairly quickly in solution on account of higher Brownian rotations. As a result, even though the catalyst may be only on one side of the sphere, the motor does not go very far in one direction before it is reoriented to travel in a different direction.

Another example of motion resulting from osmophoresis is the analyte-triggered depolymerization pump, shown in Figure 15.[84] These entropy-driven pumps consist of insoluble polymer films that depolymerize to release soluble monomeric products when exposed to a specific analyte. The pumps are self-powered: products formed as a result of the depolymerization reaction create a concentration gradient that pumps fluids (and particles) away from the bulk polymer owing to an osmophoretic mechanism. Since the depolymerization of a single polymer chain triggered by one analyte

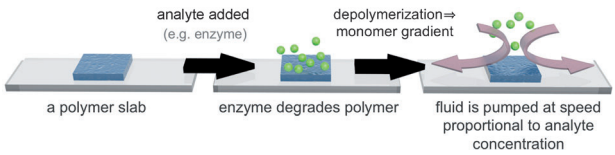

Figure 15. Insoluble polymer films respond to specific analytes (ranging from enzymes to small molecules) and depolymerize to release soluble monomeric products. This builds up a concentration gradient of the products that pumps fluids and particles away from the bulk polymer as a result of an osmophoretic mechanism. From Ref. [84].

molecule leads to a large number of monomer products, there is considerable signal amplification. The pumps are capable of turning on in response to specific analytes and can be tuned to respond to a variety of analytes, ranging from small molecules to enzymes.

Each of the two mechanisms just described (electrolyte and non-electrolyte diffusiophoresis) has its own set of advantages. Non-electrolyte diffusiophoresis has no dependence on surface charge and is able to function in high-ionic-strength media. Electrolyte diffusiophoresis, however, is not effective in high-ionic-strength media because of the collapse of the double-layer on the particle surface. Conversely, in a low-ionic-strength medium electrolyte diffusiophoresis is a more powerful mechanism, resulting in higher particle speeds. Both mechanisms occur by the chemical species responsible for the gradient being attracted to the surface either by electrostatic (electrolyte) or through van der Waals (non-electrolyte) interactions. If these two effects are comparable, the electrolyte diffusiophoresis is stronger because it has an additional electric field term [Eq. (4)].

3.5. Chemotaxis

Chemotaxis is a common phenomenon observed in biological systems and recently it has been shown in some nonbiological systems as well.[30b,83,85] Unlike biological systems, the mechanism for chemotaxis is not well understood in the latter systems. According to a hypothesis put forth by Velegol and Sen,[85] when a catalytic motor experiences different diffusivities at different substrate (fuel) concentrations, it will chemotax towards areas of higher diffusivity. Movement occurs in this direction because with higher diffusivity the motor experiences a higher average displacement so it will continue to move farther as it travels up the gradient. This was demonstrated experimentally by the authors by placing Pt–Au nanorods in a gradient of hydrogen peroxide. Over time the density of the rods began to increase in the area of the highest concentration of hydrogen peroxide (where the diffusivity was highest). In another example, when the polymerization motors described above were placed in a concentration gradient of the monomer, the density of motor particles increased with time in the area of highest monomer concentration.[83] The schooling and predator–prey behavior described in Section 3.3 are examples of chemotaxis in response to ion gradients.[76,77] In abiotic chemotaxis, it appears that the substrate gradient is somewhat analogous to a Brownian ratchet; many molecular machines in living systems function as Brownian ratchets.[20]

4. Conclusion

The rapidlyt expanding field of self-powered autonomous nano- and micromotors is still in its infancy. If one compares the current stage of reseach on nano- and micromotors to more familiar technologies, we are somewhere between the discovery of the wheel and the Industrial Revolution. The first examples of nano/micro-objects outside living systems that

move autonomously by converting chemical energy into mechanical force have been discovered. With very little information input (in the form of chemical or light gradients), these objects begin to display emergent collective behavior (simple chemotaxis,[30b,83,85] schooling,[76,77,79,80] predator–prey behavior[76]) that was thought to lie solely in the realm of biology. There is great richness in the behavior of these abiotic systems, both at the single-motor and at the ensemble level. The following scientific issues in this area need to be fully elucidated:

1. What are the possible mechanisms for momentum creation and how efficient are they in different environments?
2. Are there optimal motor geometries for sustaining orientation?
3. What gives rise to directional motion: sensing, taxis, and Levy walk[86]? Free energy expenditure is clearly required; for example, taxis is seen only when the spatially inhomogeneous diffusion lacks microscopic reversibilit.y
4. What are the ensemble properties of non-interacting super-diffusing motors?
5. What are the mechanisms of motor–motor interactions?
6. What are the ensemble dynamics? Are there analogues to phase transitions? How is the nonlinear dynamics realized?

Clearly, a close synergy between theory and experiments is required to address most of these issues. One of the exciting aspects of reseach in this area is that it draws upon the expertise from many different fields ranging from chemistry, physics, and biology to engineering.

Freed of usual biological constraints, we now have the unprecedented opportunity to probe the ultimate limits of self-organization in these dynamic systems that operate far from equilibrium. In addition, the observation in abiotic systems of behaviors previously associated with evolution-derived biological processes raises an intriguing question: Are there underlying emergent physical rules that govern both? A striking recent observation in this context is that momentum transfer from active swimmers to tracer particles shows identical scaling for bacteria and Pt–Au nanorods, meaning that the physics of particle interactions is relatively insensitive to the propulsion mechanism.[87]

Finally, by Galilean inverse, an object that moves by generating a continuous surface force in a fluid can, in principle, be used to pump the fluid by the same catalytic mechanism. Thus, by immobilizing the nano/micromotors, nano/microfluidic pumps that transduce energy catalytically have been developed.[17,67,79,84,88] These pumps are capable of moving fluids and micron-scale particles autonomously with velocities that are dictated by the concentration of the specific analyte that turns "on" the pump.[84] Thus, one can envision self-powered nonmechanical pumps that sense a specific analyte and deliver a cargo to a specific site in response. Such autonomous pumps are required for the next generation of smart micro/nanoscale devices.

Returning to the theme of the "Fantastic Voyage", while much needs to be accomplished, we are beginning to address the grand scientific challenge of understanding how to manipulate energy and information at the nanoscale.[89] This will allow us to build truly intelligent systems and create technologies that rival those of living organisms.

We thank all the Penn State faculty and students involved in catalytic motors research for many enlightening discussions. We gratefully acknowledge NSF ((DMR-0820404, CBET-1014673), and AFoSR (FA9550-10-1-0509) for supporting our current research.

Received: March 14, 2012
Revised: May 4, 2012

[1] a) *Fantastic Voyage*, S. David, Producer, Twentieth Century Fox Film Corporation, **1966**; b) M. Crichton, *Prey*, Harper Collins, New York, **2002**.
[2] E. Masayoshi, O. Takahito, *J. Phys. D* **2005**, *38*, R223.
[3] R. Feynman, *Eng. Sci.* **1960**, *23*, 22–36.
[4] R. A. Freitas, *Int. J. Surg.* **2005**, *3*, 243–246.
[5] K. Ishiyama, M. Sendoh, K. I. Arai, *J. Magn. Magn. Mater.* **2002**, *242–245*, 41–46.
[6] B. J. Nelson, I. K. Kaliakatsos, J. J. Abbott, *Annu. Rev. Biomed. Eng.* **2010**, *12*, 55–85.
[7] T. Hogg, R. A. Freitas, *Nanomedicine* **2010**, *6*, 298–317.
[8] S. Klumpp, *Physica A* **2005**, *352*, 53–112.
[9] a) M. Schliwa, G. Woehlke, *Nature* **2003**, *422*, 759–765; b) C. Mavroidis, A. Dubey, M. L. Yarmush, *Annu. Rev. Biomed. Eng.* **2004**, *6*, 363–395.
[10] B. Alberts, D. Bray, K. Hopkin, A. Hohnson, J. Lewis, M. Raff, K. Roberts, P. Walter, A. Johnson, *Essential Cell Biology*, Garland, London, **2010**.
[11] M. J. McBride, *Annu. Rev. Microbiol.* **2001**, *55*, 49–75.
[12] L. A. Dunbar, M. J. Caplan, *Eur. J. Cell Biol.* **2000**, *79*, 557–563.
[13] J. Lyklema, *Colloids Surf. A* **2003**, *222*, 5–14.
[14] T. Vickrey, J. Garcia-Ramirez, *Sep. Sci. Technol.* **1980**, *15*, 1297–1304.
[15] S. Iacopini, R. Rusconi, R. Piazza, *Eur. Phys. J. E* **2006**, *19*, 59–67.
[16] M. M. J. Lin, D. C. Prieve, *J. Colloid Interface Sci.* **1983**, *95*, 327–339.
[17] W. F. Paxton, P. T. Baker, T. R. Kline, Y. Wang, T. E. Mallouk, A. Sen, *J. Am. Chem. Soc.* **2006**, *128*, 14881–14888.
[18] W. Liu, X. Sun, H. Han, M. Li, X.-Z. Zhao, *Appl. Phys. Lett.* **2006**, *89*, 163122–163123.
[19] M. N. Vinothan, *Solid State Commun.* **2006**, *139*, 557–561.
[20] a) E. R. Kay, D. A. Leigh, F. Zerbetto, *Angew. Chem.* **2007**, *119*, 72–196; *Angew. Chem. Int. Ed.* **2007**, *46*, 72–191; b) R. D. Astumian, *Annu. Rev. Biophys.* **2011**, *40*, 289–313; c) R. D. Astumian, *Science* **1997**, *276*, 917–922; d) R. D. Astumian, *Sci. Am.* **2001**, *285*(1), 56–64; e) P. Reimann, *Phys. Rep.* **2002**, *361*, 57–265.
[21] a) G. Taylor, *Philos. Trans. R. Soc. London Ser. A* **1923**, 55; b) http://www.youtube.com/watch?v=p08_KlTKP50 (accessed March 2012).
[22] E. M. Purcell, *Am. J. Phys.* **1977**, *45*, 3–11.
[23] a) Y. Mei, A. A. Solovev, S. Sanchez, O. G. Schmidt, *Chem. Soc. Rev.* **2011**, *40*, 2109–2119; b) T. Mirkovic, N. S. Zacharia, G. D. Scholes, G. A. Ozin, *Small* **2010**, *6*, 159–167; c) T. Mirkovic, N. S. Zacharia, G. D. Scholes, G. A. Ozin, *ACS Nano* **2010**, *4*, 1782–1789; d) S. J. Ebbens, J. R. Howse, *Soft Matter* **2010**, *6*, 726–738; e) J. Wang, *ACS Nano* **2009**, *3*, 4–9; f) Y. Hong, D. Velegol, N. Chaturvedi, A. Sen, *Phys. Chem. Chem. Phys.* **2010**, *12*, 1423–1435; g) A. Sen, M. Ibele, Y. Hong, D. Velegol, *Faraday Discuss.* **2009**, *143*, 15–27; h) S. Sánchez, M. Pumera, *Chem. Asian J.* **2009**, *4*, 1402–1410.
[24] A. Goel, V. Vogel, *Nat. Nanotechnol.* **2008**, *3*, 465–475.

[25] J. Kim, J. Park, S. Yang, J. Baek, B. Kim, S. H. Lee, E.-S. Yoon, K. Chun, S. Park, *Lab Chip* **2007**, *7*, 1504 – 1508.
[26] B. Behkam, M. Sitti, *Appl. Phys. Lett.* **2007**, *90*, 023902.
[27] R. K. Soong, G. D. Bachand, H. P. Neves, A. G. Olkhovets, H. G. Craighead, C. D. Montemagno, *Science* **2000**, *290*, 1555 – 1558.
[28] C. Brunner, C. Wahnes, V. Vogel, *Lab Chip* **2007**, *7*, 1263 – 1271.
[29] a) H. Jia, G. Zhu, P. Wang, *Biotechnol. Bioeng.* **2003**, *84*, 406 – 414; b) N. Mano, A. Heller, *J. Am. Chem. Soc.* **2005**, *127*, 11574 – 11575; c) D. Pantarotto, W. R. Browne, B. L. Feringa, *Chem. Commun.* **2008**, 1533 – 1535.
[30] a) H. S. Muddana, S. Sengupta, T. E. Mallouk, A. Sen, P. J. Butler, *J. Am. Chem. Soc.* **2010**, *132*, 2110 – 2111; b) H. Yu, K. Jo, K. L. Kounovsky, J. J. d. Pablo, D. C. Schwartz, *J. Am. Chem. Soc.* **2009**, *131*, 5722 – 5723.
[31] D. Brady, J. Jordaan, *Biotechnol. Lett.* **2009**, *31*, 1639 – 1650.
[32] J. L. Anderson, *Ann. N. Y. Acad. Sci.* **1986**, *469*, 166 – 177.
[33] W. F. Paxton, K. C. Kistler, C. C. Olmeda, A. Sen, S. K. St. Angelo, Y. Cao, T. E. Mallouk, P. E. Lammert, V. H. Crespi, *J. Am. Chem. Soc.* **2004**, *126*, 13424 – 13431.
[34] S. Fournier-Bidoz, A. C. Arsenault, I. Manners, G. A. Ozin, *Chem. Commun.* **2005**, 441 – 443.
[35] R. F. Ismagilov, A. Schwartz, N. Bowden, G. M. Whitesides, *Angew. Chem.* **2002**, *114*, 674 – 676; *Angew. Chem. Int. Ed.* **2002**, *41*, 652 – 654.
[36] a) L. Rayleigh, *Proc. R. Soc. London* **1890**, *47*, 364 – 367; b) S. Nakata, S.-i. Hiromatsu, H. Kitahata, *J. Phys. Chem. B* **2003**, *107*, 10557 – 10559; c) O. Sano, K. Kutsumi, N. Watanabe, *J. Phys. Soc. Jpn.* **1995**, *64*, 1993 – 1999; d) Y. Sumino, N. Magome, T. Hamada, K. Yoshikawa, *Phys. Rev. Lett.* **2005**, *94*, 068301; e) M. M. Hanczyc, T. Toyota, T. Ikegami, N. Packard, T. Sugawara, *J. Am. Chem. Soc.* **2007**, *129*, 9386 – 9389; f) I. Lagzi, S. Soh, P. J. Wesson, K. P. Browne, B. A. Grzybowski, *J. Am. Chem. Soc.* **2010**, *132*, 1198 – 1199.
[37] a) W. F. Paxton, A. Sen, T. E. Mallouk, *Chem. Eur. J.* **2005**, *11*, 6462 – 6470; b) J. L. Moran, J. D. Posner, *J. Fluid Mech.* **2011**, *680*, 31 – 66.
[38] Y. Wang, R. M. Hernandez, D. J. Bartlett, J. M. Bingham, T. R. Kline, A. Sen, T. E. Mallouk, *Langmuir* **2006**, *22*, 10451 – 10456.
[39] N. Kocherginsky, *Prog. Biophys. Mol. Biol.* **2009**, *99*, 20 – 41.
[40] R. Liu, A. Sen, *J. Am. Chem. Soc.* **2011**, *133*, 20064 – 20067.
[41] a) G. Loget, A. Kuhn, *J. Am. Chem. Soc.* **2010**, *132*, 15918 – 15919; b) G. Loget, A. Kuhn, *Nat. Commun.* **2011**, *2*, 535.
[42] U. K. Demirok, R. Laocharoensuk, K. M. Manesh, J. Wang, *Angew. Chem.* **2008**, *120*, 9489 – 9491; *Angew. Chem. Int. Ed.* **2008**, *47*, 9349 – 9351.
[43] R. Laocharoensuk, J. Burdick, J. Wang, *ACS Nano* **2008**, *2*, 1069 – 1075.
[44] a) D. Kagan, P. Calvo-Marzal, S. Balasubramanian, S. Sattayasamitsathit, K. M. Manesh, G.-U. Flechsig, J. Wang, *J. Am. Chem. Soc.* **2009**, *131*, 12082 – 12083; b) S. Sattayasamitsathit, W. Gao, P. Calvo-Marzal, K. M. Manesh, J. Wang, *ChemPhysChem* **2010**, *11*, 2802 – 2805.
[45] S. Balasubramanian, D. Kagan, K. M. Manesh, P. Calvo-Marzal, G.-U. Flechsig, J. Wang, *Small* **2009**, *5*, 1569 – 1574.
[46] P. Calvo-Marzal, K. M. Manesh, D. Kagan, S. Balasubramanian, M. Cardona, G.-U. Flechsig, J. Posner, J. Wang, *Chem. Commun.* **2009**, 4509 – 4511.
[47] a) W. Gao, S. Sattayasamitsathit, K. M. Manesh, D. Weihs, J. Wang, *J. Am. Chem. Soc.* **2010**, *132*, 14403 – 14405; b) W. Gao, K. M. Manesh, J. Hua, S. Sattayasamitsathit, J. Wang, *Small* **2011**, *7*, 2047 – 2051.
[48] O. S. Pak, W. Gao, J. Wang, E. Lauga, *Soft Matter* **2011**, *7*, 8169 – 8181.
[49] N. S. Zacharia, Z. S. Sadeq, G. A. Ozin, *Chem. Commun.* **2009**, 5856 – 5858.
[50] J. Wu, S. Balasubramanian, D. Kagan, K. M. Manesh, S. Campuzano, J. Wang, *Nat. Commun.* **2010**, *1*, 36.
[51] T. R. Kline, W. F. Paxton, T. E. Mallouk, A. Sen, *Angew. Chem.* **2005**, *117*, 754 – 756; *Angew. Chem. Int. Ed.* **2005**, *44*, 744 – 746.
[52] a) D. Kagan, R. Laocharoensuk, M. Zimmerman, C. Clawson, S. Balasubramanian, D. Kang, D. Bishop, S. Sattayasamitsathit, L. Zhang, J. Wang, *Small* **2010**, *6*, 2741 – 2747; b) S. Sundararajan, P. E. Lammert, A. W. Zudans, V. H. Crespi, A. Sen, *Nano Lett.* **2008**, *8*, 1271 – 1276.
[53] a) J. Burdick, R. Laocharoensuk, P. M. Wheat, J. D. Posner, J. Wang, *J. Am. Chem. Soc.* **2008**, *130*, 8164 – 8165; b) S. Sundararajan, S. Sengupta, M. E. Ibele, A. Sen, *Small* **2010**, *6*, 1479 – 1482.
[54] P. Calvo-Marzal, S. Sattayasamitsathit, S. Balasubramanian, J. R. Windmiller, C. Dao, J. Wang, *Chem. Commun.* **2010**, *46*, 1623 – 1624.
[55] J. Orozco, S. Campuzano, D. Kagan, M. Zhou, W. Gao, J. Wang, *Anal. Chem.* **2011**, *83*, 7962 – 7969.
[56] J. M. Catchmark, S. Subramanian, A. Sen, *Small* **2005**, *1*, 202 – 206.
[57] a) L. Qin, M. J. Banholzer, X. Xu, L. Huang, C. A. Mirkin, *J. Am. Chem. Soc.* **2007**, *129*, 14870 – 14871; b) Y. Wang, S.-t. Fei, Y.-M. Byun, P. E. Lammert, V. H. Crespi, A. Sen, T. E. Mallouk, *J. Am. Chem. Soc.* **2009**, *131*, 9926 – 9927; c) Y. He, J. Wu, Y. Zhao, *Nano Lett.* **2007**, *7*, 1369 – 1375.
[58] B. R. Martin, D. J. Dermody, B. D. Reiss, M. Fang, L. A. Lyon, M. J. Natan, T. E. Mallouk, *Adv. Mater.* **1999**, *11*, 1021 – 1025.
[59] L. M. Goldenberg, J. Wagner, J. Stumpe, B.-R. Paulke, E. Görnitz, *Langmuir* **2002**, *18*, 5627 – 5629.
[60] a) J. R. Howse, R. A. L. Jones, A. J. Ryan, T. Gough, R. Vafabakhsh, R. Golestanian, *Phys. Rev. Lett.* **2007**, *99*, 048102; b) L. F. Valadares, Y.-G. Tao, N. S. Zacharia, V. Kitaev, F. Galembeck, R. Kapral, G. A. Ozin, *Small* **2010**, *6*, 565 – 572; c) H. Ke, S. Ye, R. L. Carroll, K. Showalter, *J. Phys. Chem. A* **2010**, *114*, 5462 – 5467; d) L. Baraban, D. Makarov, R. Streubel, I. Monch, D. Grimm, S. Sanchez, O. G. Schmidt, *ACS Nano* **2012**, DOI: 10.1021/nn300413p.
[61] See Ref. [32].
[62] J. G. Gibbs, S. Kothari, D. Saintillan, Y. P. Zhao, *Nano Lett.* **2011**, *11*, 2543 – 2550.
[63] a) Y. Mei, G. Huang, A. A. Solovev, E. B. Ureña, I. Mönch, F. Ding, T. Reindl, R. K. Y. Fu, P. K. Chu, O. G. Schmidt, *Adv. Mater.* **2008**, *20*, 4085 – 4090; b) K. M. Manesh, M. Cardona, R. Yuan, M. Clark, D. Kagan, S. Balasubramanian, J. Wang, *ACS Nano* **2010**, *4*, 1799 – 1804.
[64] S. Sanchez, A. A. Solovev, Y. Mei, O. G. Schmidt, *J. Am. Chem. Soc.* **2010**, *132*, 13144 – 13145.
[65] S. Sanchez, A. A. Solovev, S. M. Harazim, O. G. Schmidt, *J. Am. Chem. Soc.* **2011**, *133*, 701 – 703.
[66] A. A. Solovev, Y. Mei, O. G. Schmidt, *Adv. Mater.* **2010**, *22*, 4340 – 4344.
[67] A. A. Solovev, S. Sanchez, Y. Mei, O. G. Schmidt, *Phys. Chem. Chem. Phys.* **2011**, *13*, 10131 – 10135.
[68] a) S. Sanchez, A. A. Solovev, S. Schulze, O. G. Schmidt, *Chem. Commun.* **2011**, *47*, 698 – 700; b) A. A. Solovev, S. Sanchez, M. Pumera, Y. F. Mei, O. G. Schmidt, *Adv. Funct. Mater.* **2010**, *20*, 2430 – 2435; c) A. A. Solovev, W. Xi, D. H. Gracias, S. M. Harazim, C. Deneke, S. Sanchez, O. G. Schmidt, *ACS Nano* **2012**, *6*, 1751 – 1756.
[69] D. Kagan, S. Campuzano, S. Balasubramanian, F. Kuralay, G.-U. Flechsig, J. Wang, *Nano Lett.* **2011**, *11*, 2083 – 2087.
[70] S. Balasubramanian, D. Kagan, C.-M. Jack Hu, S. Campuzano, M. J. Lobo-Castañon, N. Lim, D. Y. Kang, M. Zimmerman, L. Zhang, J. Wang, *Angew. Chem.* **2011**, *123*, 4247 – 4250; *Angew. Chem. Int. Ed.* **2011**, *50*, 4161 – 4164.
[71] S. Sanchez, A. N. Ananth, V. M. Fomin, M. Viehrig, O. G. Schmidt, *J. Am. Chem. Soc.* **2011**, *133*, 14860 – 14863.

[72] A. A. Solovev, E. J. Smith, C. C. Bof'Bufon, S. Sanchez, O. G. Schmidt, *Angew. Chem.* **2011**, *123*, 11067 – 11070; *Angew. Chem. Int. Ed.* **2011**, *50*, 10875 – 10878.
[73] W. Gao, S. Sattayasamitsathit, J. Orozco, J. Wang, *J. Am. Chem. Soc.* **2011**, *133*, 11862 – 11864.
[74] a) K. K. Dey, D. Sharma, S. Basu, A. Chattopadhyay, *J. Chem. Phys.* **2008**, *129*, 121101 – 121104; b) K. K. Dey, K. K. Senapati, P. Phukan, S. Basu, A. Chattopadhyay, *J. Phys. Chem. C* **2011**, *115*, 12708 – 12715.
[75] J. L. Anderson, *Annu. Rev. Fluid Mech.* **1989**, *21*, 61 – 99.
[76] M. Ibele, T. E. Mallouk, A. Sen, *Angew. Chem.* **2009**, *121*, 3358 – 3362; *Angew. Chem. Int. Ed.* **2009**, *48*, 3308 – 3312.
[77] M. E. Ibele, P. E. Lammert, V. H. Crespi, A. Sen, *ACS Nano* **2010**, *4*, 4845 – 4851.
[78] J. L. Anderson, *Ann. N. Y. Acad. Sci.* **1986**, *469*, 166 – 177.
[79] Y. Hong, M. Diaz, U. M. Córdova-Figueroa, A. Sen, *Adv. Funct. Mater.* **2010**, *20*, 1568 – 1576.
[80] D. Kagan, S. Balasubramanian, J. Wang, *Angew. Chem.* **2011**, *123*, 523 – 526; *Angew. Chem. Int. Ed.* **2011**, *50*, 503 – 506.
[81] N. Chaturvedi, Y. Y. Hong, A. Sen, D. Velegol, *Langmuir* **2010**, *26*, 6308 – 6313.
[82] a) R. Golestanian, T. B. Liverpool, A. Ajdari, *Phys. Rev. Lett.* **2005**, *94*, 220801; b) G. Rückner, R. Kapral, *Phys. Rev. Lett.* **2007**, *98*, 150603; c) U. M. Córdova-Figueroa, J. F. Brady, *Phys. Rev. Lett.* **2008**, *100*, 158303; d) F. Delogu, *J. Phys. Chem. C* **2009**, *113*, 15909 – 15913; e) S. Ebbens, R. A. L. Jones, A. J. Ryan, R. Golestanian, J. R. Howse, *Phys. Rev. E* **2010**, *82*, 015304; f) M. N. Popescu, S. Dietrich, M. Tasinkevych, J. Ralston, *Eur. Phys. J. E* **2010**, *31*, 351 – 367.
[83] R. A. Pavlick, S. Sengupta, T. McFadden, H. Zhang, A. Sen, *Angew. Chem.* **2011**, *123*, 9546 – 9549; *Angew. Chem. Int. Ed.* **2011**, *50*, 9374 – 9377.
[84] H. Zhang, K. Yeung, J. S. Robbins, R. A. Pavlick, M. Wu, R. Liu, A. Sen, S. T. Phillips, *Angew. Chem.* **2012**, *124*, 2450 – 2454; *Angew. Chem. Int. Ed.* **2012**, *51*, 2400 – 2404.
[85] Y. Hong, N. M. K. Blackman, N. D. Kopp, A. Sen, D. Velegol, *Phys. Rev. Lett.* **2007**, *99*, 178103.
[86] P. Dhar, T. M. Fischer, Y. Wang, T. E. Mallouk, W. F. Paxton, A. Sen, *Nano. Lett.* **2006**, *6*, 66 – 72.
[87] G. Mino, T. E. Mallouk, T. Darnige, M. Hoyos, J. Dauchet, J. Dunstan, R. Soto, Y. Wang, A. Rousselet, E. Clement, *Phys. Rev. Lett.* **2011**, *106*, 048102.
[88] a) A. Nisar, N. Afzulpurkar, B. Mahaisavariya, A. Tuantranont, *Sens. Actuators B* **2008**, *130*, 917 – 942; b) T. R. Kline, W. F. Paxton, Y. Wang, D. Velegol, T. E. Mallouk, A. Sen, *J. Am. Chem. Soc.* **2005**, *127*, 17150 – 17151; c) M. E. Ibele, Y. Wang, T. R. Kline, T. E. Mallouk, A. Sen, *J. Am. Chem. Soc.* **2007**, *129*, 7762 – 7763; d) I. K. Jun, H. Hess, *Adv. Mater.* **2010**, *22*, 4823 – 4825.
[89] http://science.energy.gov/bes/efrc/research/grand-challenges/.